Received: 20 September 2022 | Accepted: 21 November 2022

DOI: 10.1002/biof.1922

RESEARCH ARTICLE

Biofactors WILEY

Rosa gallica and its active compound, cyanidin-3,5-*O*-diglucoside, improve skin hydration via the GLK signaling pathway

Ji-Won Seo[1] | **Seongin Jo**[2] | **Young Sung Jung**[3] | **Mohammad-Al Mijan**[4] | **Joy Cha**[5] | **Seungpyo Hong**[6] | **Sanguine Byun**[2] | **Tae-Gyu Lim**[4,7,8]

[1]Department of Agricultural Biotechnology and Research Institute of Agriculture and Life Sciences, Seoul National University, Seoul, Republic of Korea

[2]Department of Biotechnology, Yonsei University, Seoul, Republic of Korea

[3]Korea Food Research Institute, Wanju-gun, Republic of Korea

[4]Department of Food Science and Biotechnology, Sejong University, Seoul, Republic of Korea

[5]Division of Bioengineering, Incheon National University, Incheon, Republic of Korea

[6]Department of Molecular Biology, Jeonbuk National University, Jeonju, Republic of Korea

[7]R&D Center, NOVAWells Co., Ltd., Cheongju, South Korea

[8]Department of Food Science and Biotechnology, and Carbohydrate Bioproduct Research Center, Sejong University, Seoul, Republic of Korea

Correspondence
Tae-Gyu Lim, Department of Food Science and Biotechnology, Sejong University, Seoul 05006, Republic of Korea.
Email: tglim@sejong.ac.kr

Sanguine Byun, Department of Biotechnology, Yonsei University, Seoul 03722, Republic of Korea.
Email: sanguine@yonsei.ac.kr

Funding information
Korea Institute of Planning and Evaluation for Technology in Food, Agriculture, Forestry and Fisheries, Grant/Award Number: 821018f3; Ministry of SMEs and Startups, Grant/Award Number: S3094265; National Research Foundation of Korea, Grant/Award Number: 2020R1A2C1010703

Abstract

Rosa gallica has been previously reported to display anti-inflammatory, anti-oxidative, and anti-skin wrinkle activities. However, the effect of *Rosa gallica* on skin hydration and its active components are largely unknown. Herein, we aimed to investigate the skin hydration effect of rose petal extract (RPE) in humans and elucidate the underlying molecular mechanism. A double-blinded clinical study was performed to investigate the effect of RPE on skin hydration. Stratum corneum moisture analysis demonstrated that RPE treatment significantly improved hydration levels in human skin. Furthermore, HAS2 and hyaluronic acid levels were notably increased by RPE in keratinocytes and 3D human skin equivalent model. By comparing the modulatory effect on HAS2 expression, cyanidin-3,5-*O*-diglucoside (CDG) was identified as the most potent compound in RPE likely responsible for skin hydration. The kinase activity of GLK, an upstream regulator of MAPK signaling, was increased by CDG in a dose-dependent manner. Importantly, silencing GLK reversed CDG-mediated HAS2 upregulation, further supporting the involvement of GLK in the CDG-mediated effects. Binding of CDG to GLK was confirmed by pull-down assay and computer modeling. These findings suggest that RPE and its active

Abbreviations: CDG, cyanidin-3,5-*O*-diglucoside; DMEM, Dulbecco's Modified Eagle Medium; ECM, extracellular matrix; FBS, fetal bovine serum; GLK, germinal-center kinase-like kinase; HA, hyaluronic acid; HAS, hyaluronic acid synthase; IHC, immunohistochemistry; MAPKs, mitogen-activated protein kinase; RPE, *Rosa gallica* petal extract.

Ji-Won Seo and Seongin Jo contributed equally to this study.

component CDG increases skin hydration by upregulating HAS2 expression through modulating the GLK-MAP2K-MAPK signaling pathway.

KEYWORDS

cyanidin-3,5-*O*-diglucoside, GLK, HAS2, hyaluronic acid, *Rosa gallica*, skin hydration

1 | INTRODUCTION

As the largest and most external organ of the human body, the skin provides a selective barrier and protects our body from external insults. To maintain its proper function and biophysical characteristics, skin requires an adequate level of hydration.[1] Lack of moisture in the skin can lead to physiological dysfunction and deterioration of its physical appearance.[2,3] Hyaluronic acid (HA), the major molecule present in the extracellular matrix (ECM) of the skin, has been the focus of research for its exquisite role in maintaining skin hydration and elasticity.[4,5] HA is a high-molecular-mass linear polysaccharide composed of repeatedly arranged N-acetylglucosamine and glucoronic acid. The average human body is estimated to contain 15 g of HA, of which 50% is ubiquitously distributed in the skin, with the rest mostly present in the bone cartilage.[6,7] The key feature of this molecule is that it can retain moisture more than 1000 times its weight.[8]

HA is synthesized at the interior of the plasma membrane by an enzyme called hyaluronic acid synthase (HAS). It has three isoforms, namely HAS1, HAS2, and HAS3, and is later translocated into the ECM.[9] Both HAS2 and HAS3 actively participate in HA synthesis, with HAS2 generally acting inside keratinocytes while HAS3 acts in the epidermis.[10]

Reportedly, the upregulation of HAS enzymes and the production of HA is heavily reliant upon the activation of mitogen-activated protein kinase (MAPKs), including p38 and ERK.[7,11] Germinal-center kinase-like kinase (GLK), also known as MAP4K3, is regarded as one of the key modulators of MAPK signaling.[12] It has been reported that GLK phosphorylation can regulate downstream signaling cascades, including MAP2Ks/JNK and MAPKs (MAP4K3 family kinases in immunity and inflammation). Moreover, GLK has been reported as an anti-aging regulator in mouse studies.[13] It is therefore plausible that GLK could have a positive impact on the moisture and the integrity of human skin.

Beyond their medicinal applications, rose petals and rose essential oils have been reported as potent skin-care ingredients in previous studies.[14,15] In a recent investigation by our group, rose petal extract (RPE) from *Rosa gallica* enabled remarkable skin whitening and anti-wrinkle effects.[16,17] Despite being a potential beauty ingredient, the skin moisturizing effects of RPE have not yet been investigated. We sought to investigate the skin hydration efficacies of RPE and the underlying molecular mechanisms involved with a clinical trial and by using a 3D human skin equivalent model and human keratinocytes.

2 | MATERIALS AND METHODS

2.1 | Rose petal extract

Rosa gallica petals grown in Turkey were provided through GN Bio (Hannam, Korea). RPE was prepared as described previously.[15] Briefly, 10 g of dried rose petal powder was extracted with 1000 ml of 70% ethanol at 70°C for 3 h using a reflux condenser. The extracted solution was filtered through a Whatman No.2 filter paper (Whatman, Maidstone, UK). The solvent was lyophilized in a freeze dryer and kept at −20°C.

2.2 | Subjects and test substance for clinical study

Female volunteers aged between 20 and 60 years were recruited for this study. The study was approved by the local medical ethics committee (permit number KIDS-BTE003-SJU) and conducted following the principles of the Declaration of Helsinki. RPE-containing cream was applied to the left half of the face and a control cream with identical formulation but without RPE was applied to the right half of the face as a vehicle control. The treatment was performed once daily after washing the face.

2.3 | Assessment of skin moisture retention

An Epsilon E100 (Biox Systems Ltd., UK) was used to assess skin moisture retention. Participants were acclimatized for 30 min prior to the measurement under ambient conditions with a constant temperature of 22 ± 2°C and a relative humidity of 50 ± 5%. The same researcher measured both cheeks of all subjects. Instrument

measurements were conducted before and after 2 and 4 weeks of applying the test substance. Wilcoxon signed-rank test and Repeated measures of ANOVA analysis were conducted to see any significant change in moisturizing improvement. Skin moisture data were analyzed using Epsilon E100 Software V3.1.

2.4 | Human skin equivalent preparation

A 3D human skin equivalent model was prepared in Neoderm-ED 12-well plates purchased from Tego Science (Seoul, Korea). The 3D human skin equivalent was pretreated with RPE (20–80 μg/mL) for 24 h for both the collection of cell lysates for Western blotting and for fixing in 4% formaldehyde for immunohistochemistry (IHC). For IHC, skin sections were created as described.[18] Slides were incubated with HAS2 (1:50 dilution) antibody at 4°C overnight. After washing in PBS, counterstaining was performed using hematoxylin. The level of HAS2 was examined under 400× magnification using an Olympus BX53 light microscope (Olympus Microscope System BX51; Olympus, Tokyo, Japan).

2.5 | Cell culture

HaCaT cells were cultured in Dulbecco's Modified Eagle Medium (DMEM) containing 10% fetal bovine serum (FBS) and penicillin (100 IU)/streptomycin (100 μg/mL) in a 5% CO_2 atmosphere at 37°C.

2.6 | Cell viability assay

Cell viability was measured with an MTS assay. HaCaT cells were cultured to confluence in 96-well plates before RPE was treated to the cells for 24 h. MTS reagents were then added followed by incubation for 1 h. The optical density of the solution was measured at 490 nm with a Cytation1 microplate reader system (BioTek, VT, USA).

2.7 | Enzyme-linked immunosorbent assay for HA content

HA concentrations in the keratinocytes were measured with a Hyaluronic acid DuoSet ELISA kit (R&D systems Inc., MN, USA) following the manufacturer's instructions.

2.8 | Western blot

Protein was extracted with lysis buffer (Cell Signaling Technology, Beverly, MA, USA) and concentrations were measured with a BCA assay (Pierce Biotechnology, Waltham, MA, USA). Western blotting was conducted as described previously.[7] Protein bands were detected with a chemiluminescence imaging system (Atto, Taito-ku, Tokyo, Japan) or an automatic X-ray film processor (JPI Helathcare, Seoul, Korea).[19] The bands were quantified using ImageJ (National Institutes of Health, Bethesda, MD).

2.9 | UPLC-PDA conditions

UPLC coupled with a PDA Chromatographic section was performed on Agilent eclipse plus RRHD Columns (1.8 μm, 2.1 mm × 100 mm), while elution was performed with 0.1% troflouracetic acid in DW/acetonitrile. The injection volume was 2 μl and the flow rate was 0.5 ml/min.

2.10 | Chemicals

Gallic acid, catechin, rutin, quercetin, and kaempferol were purchased from Sigma-Aldrich (St. Louis, MO, USA). Cyanidin-3,5-*O*-diglucoside was obtained from Extrasynthese (Genay, France).

2.11 | Kinase activity

The in vitro kinase assay was conducted using SelectScreen Kinase Profiling Services (Thermo Fisher Scientific, Massachusetts, MA, USA). Kinase assays were performed in duplicate.

2.12 | Preparation of RPE- and CDG-Sepharose 4B beads

Freeze-dried Sepharose 4B (GE Healthcare, Pittsburgh, PA) was activated in 1 mM HCl and suspended in RPE and CDG (2 mg) coupling buffer [0.1 M $NaHCO_3$ (pH 8.3) and 0.5 M NaCl]. Following overnight rotation at 4°C, the mixture was transferred to 0.1 M Tris–HCl buffer (pH 8.0) and again further rotated at 4°C overnight. The mixture was removed by washing in 0.1 M acetate buffer (pH 4.0) and 0.1 M Tris–HCl + 0.5 M NaCl buffer (pH 8.0) three times.

2.13 | Cell-based pull-down assay

HaCaT cell lysate (500 μg) was mixed with RFE-Sepharose 4B beads, CDG-Sepharose 4B beads, or Sepharose 4B alone beads. The pull-down assay was conducted as described.[20]

2.14 | Transfection with small interfering RNA

Scrambled small interfering RNA (siRNA) (SC-37007) and GLK siRNA (SC-39241) were obtained from Santa Cruz Biotechnology (Santa Cruz, CA, USA). Transient transfection of siRNA was performed using Lipofectamine (13778-100 Thermo Fisher). siRNAs (10 μM) were mixed with transfection reagent according to the instructions.

2.15 | Structure analysis and docking simulation

The structure of GLK (PDB ID: 5J5T), PRKACA with peptide inhibitor (PDB ID: 1ATP), GSK3B (PDB ID: 1GNG), FGFR2 (PDB ID: 1GJO), and LYN (PDB ID: 3A4O) were downloaded from the Protein Databank (PDB ID: 5J5T),[21] and the structure of CDG was retrieved from PubChem (PubChem CID: 441688).[22] The structures of the kinases were superimposed onto that of GLK to illustrate the putative peptide binding location using PyMOL Molecular Graphics System, Version 2.5.0 (Schrödinger, LLC, New York, NY, USA). The structures were visualized using PyMOL. GLK and CDG structures were converted into the PDBQT format using *prepare_receptor4.py* and *prepare_ligand4.py* scripts from AutoDock Tools, respectively.[23] GLK was docked in a cubic box of length 10 Å centered on the activation loop binding site using AutoDock Vina (Version 1.1.2).[24]

TABLE 1 Skin moisture assessment (human subjects)

	Control			RPE		
No.	Week 0	Week 2	Week 4	Week 0	Week 2	Week 4
1	13.5	13.63	13.75	11.24	12.9	13.37
2	16.03	17.16	17.26	16.14	18.75	21.14
3	21.6	22.38	22.38	20.75	22.18	22.72
4	17.89	18.57	18.64	18.54	20.08	22.82
5	19.72	20.02	20.55	19.63	21.41	22.18
6	18.11	19.44	21.18	17.43	18.29	20.74
7	21.17	21.33	21.43	21.55	24.81	25.72
8	19.4	19.94	21.58	16.93	20.9	21.79
9	18.39	18.91	18.92	18.16	19.69	20.58
10	19.13	19.38	21.18	19.38	21.84	23.87
11	15.38	16.59	17.11	14.82	16.79	17.68
12	18.3	18.78	20.28	18.01	20.77	22.67
13	16.29	17.59	18.18	17.6	19.12	20.97
14	13.6	13.77	13.87	13.61	15.41	16.98
15	14.7	15.92	16.33	14.79	16.44	18.99
16	19.13	19.52	19.92	20.4	21.98	23.01
17	17.46	17.61	17.82	18.14	20.23	22.62
18	20.02	21.51	21.57	18.97	21.31	22.57
19	19.2	20.29	20.4	18.23	19.45	21.05
20	17.12	17.56	18.55	16.18	17.48	19.65
21	13.83	15.29	16.03	14.66	16.94	19.07
22	19.01	19.19	19.78	19.71	20.5	22.79
23	17.25	18.94	19.29	17.01	19.11	21.8
Average	17.66	18.41	18.96	17.47	19.41	21.08
Standard deviation	2.31	2.28	2.40	2.47	2.60	2.61

Note: Skin moisture levels are displayed in arbitrary units quantified by Epsilon E 100. Hydration was measured on the cheek of each subject.

2.16 | Statistics

All experiments were conducted in triplicate and the results are expressed as mean ± standard deviation. Student's *t* test was performed to compare the data, where significance was determined at $p < 0.05$. All statistical analyses were performed using Microsoft Excel and SPSS (Chicago, IL, USA).

3 | RESULTS

3.1 | RPE improves skin hydration in human subjects

After 4 weeks of RPE treatment, hydration levels were markedly increased when compared to measurements taken prior to treatment (Table 1). Notably, increases in

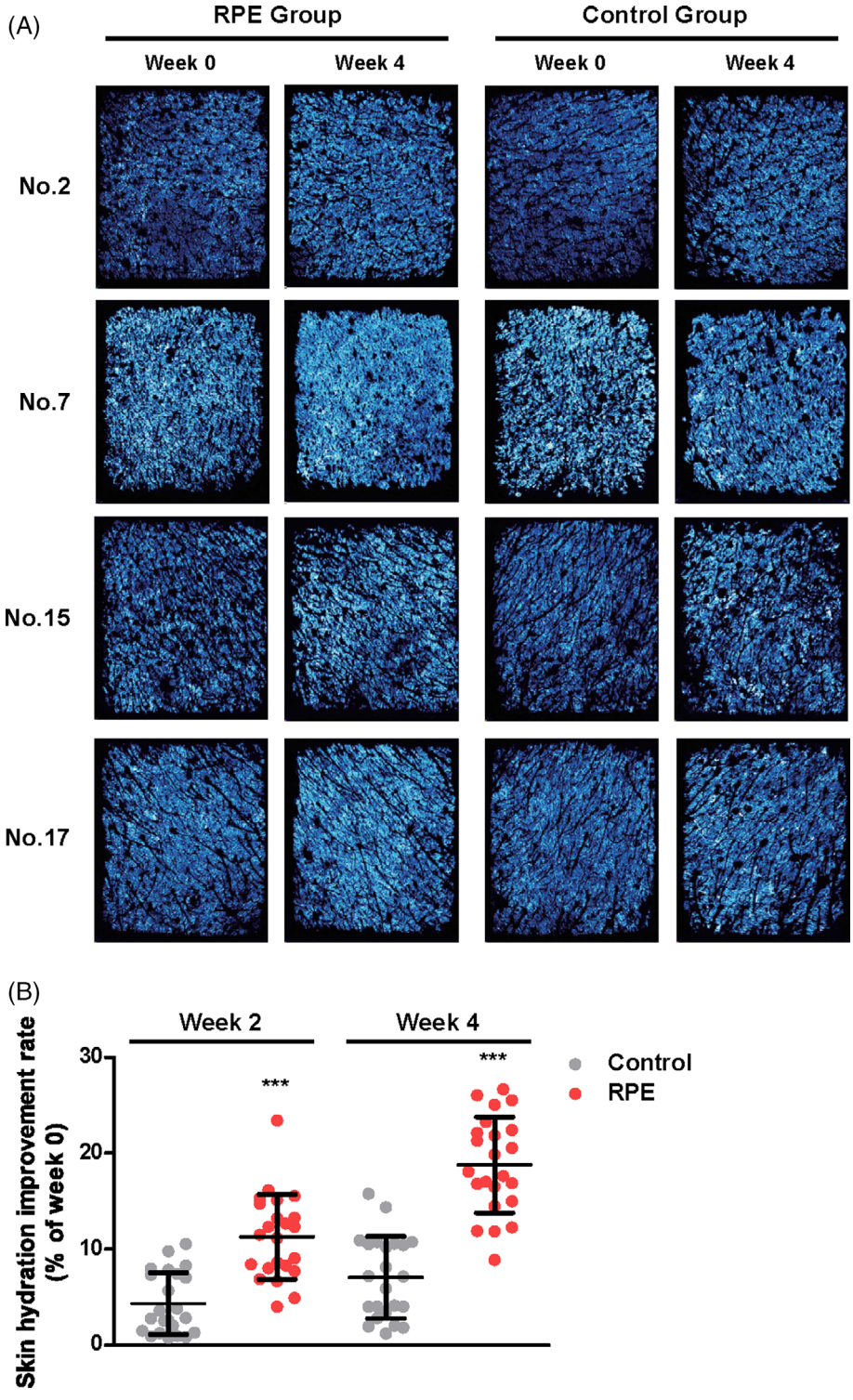

FIGURE 1 RPE increases skin hydration in human subjects. (A) Representative images of skin sections at the beginning (week 0) and at the end of the study (week 4). (B) Effects of RPE on skin moisture content. Changes in skin moisture content measured at week 2 and 4 as compared to that measured on the first day of the clinical study (i.e., week 0). Data are shown as mean ± S.D. (***$P < 0.001$, significant difference between control and RPE group.) RPE, rose petal extract

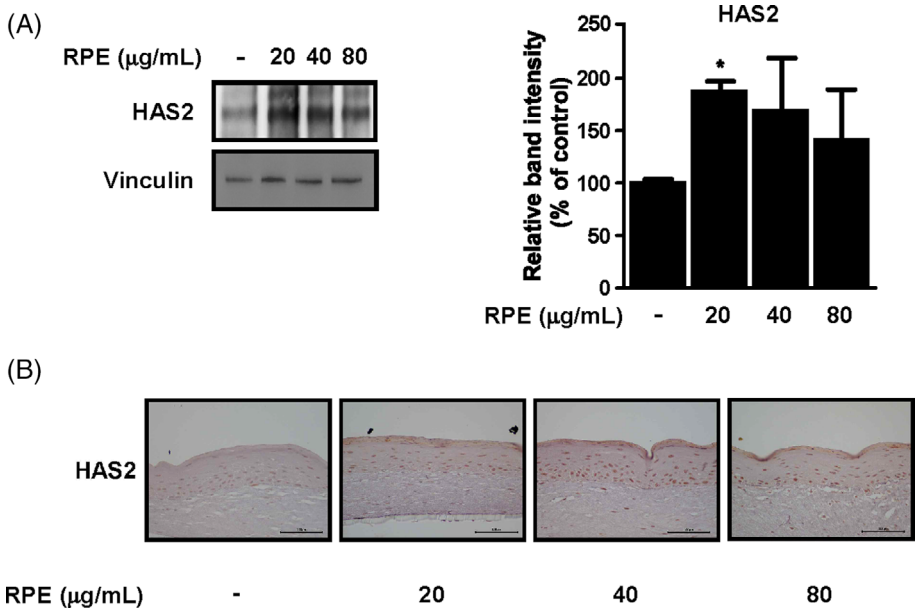

FIGURE 2 RPE increases HAS2 expression in a 3D human skin equivalent model. (A) RPE induced HAS2 expression in a 3D human skin equivalent model as determined by Western blotting. Data ($n = 3$) are mean values ± SD. (B) RPE induced HAS2 expression in a 3D human skin model obtained through immunohistochemical staining. The scale bar indicates 100 μm. Data shown as mean ± S.D (*$P < 0.05$, significant difference between control and RPE group). HAS, hyaluronic acid synthase; RPE, rose petal extract

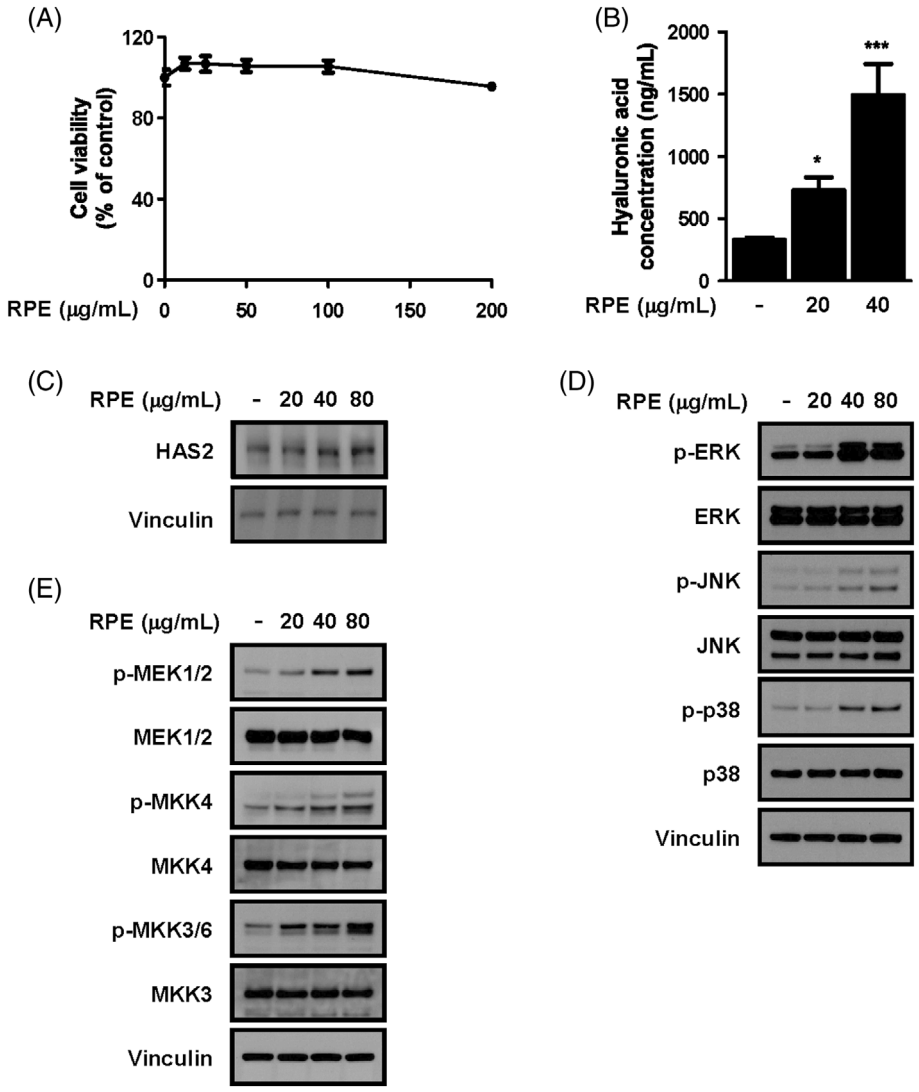

FIGURE 3 Effects of RPE on HA production and downstream signaling pathways in human keratinocytes. (A) Cell viability was measured using an MTS assay. (B) Effect of RPE on HA production in HaCaT cells. Data shown in (A) and (B) ($n = 3$) are mean values ± SD. (C) RPE increases HAS2 expression in HaCaT Cells. Cells were treated with RPE for 3 h. (D) Effects of RPE on MAPK signaling in HaCaT cells. Treating cells with RPE for 1 h induced phosphorylation of several MAPKs. (E) RPE also induced MAP2K phosphorylation in HaCaT cells. Protein expression of phosphorylated and total MAPKs, and MAP2Ks were determined by Western blot. Vinculin was used as a loading control. HA, hyaluronic acid; HAS, hyaluronic acid synthase; MAPKs, mitogen-activated protein kinase; RPE, rose petal extract

skin hydration on the RPE-treated side of the face were substantially higher than on the control-treated side. Images of the stratum corneum in the skin were taken before (week 0) and after (week 4) the treatment, with areas with low-moisture content appearing dark and areas with higher moisture content appearing relatively brighter (Figure 1A). Quantification of the data represented in Figure 1B also showed that skin hydration improvement was significantly higher (11.07% and 20.63% after 2 and 4 weeks, respectively) in the RPE group than the control group.

3.2 | RPE increases HAS2 expression in a 3D human skin equivalent model

To investigate the mechanism of action, we first attempted to examine the effect of RPE on the expression of HAS2 in a 3D human skin equivalent model. As shown in Figure 2A, HAS2 expression was markedly increased by RPE treatment compared to the control group. In support of the immunoblot findings, upregulated HAS2 expression was also observed in the immunohistochemistry analysis of tissues (Figure 2B).

TABLE 2 Quantification of major chemical constituents in RPE

Peak	Compound	t_R (min)	Avareage (mg/m)	STD
1	Gallic acid	1.191	**38.67**	1.94
2	Catechin	4.098	**32.16**	1.69
3	Rutin	7.975	**6.660**	0.228
4	Quercetin	16.652	**2.192**	0.141
5	Kaempferol	18.033	**0.471**	0.018
6	Cyanidin-3,5-*O*-diglucoside	4.348	**0.0618**	0.00106

Abbreviations: RPE, rose petal extract; t_R, retention time.

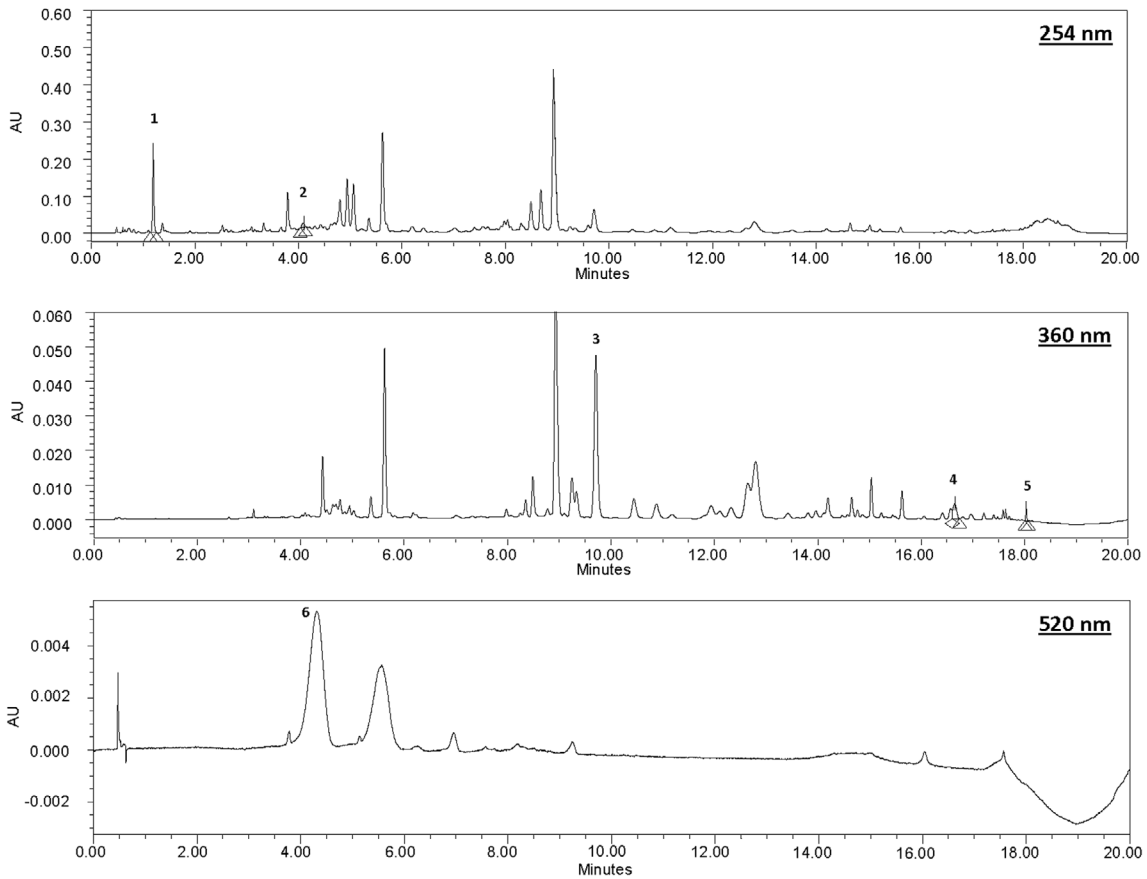

FIGURE 4 Peak intensity chromatogram of UPLC (Ultar Performance Liquid Chromatography) coupled with a PDA (Photodiode Array). Peaks are indicated in Table 2

3.3 | RPE increases HA production via modulation of the MAP2K-MAPK pathways

We next investigated the underlying molecular mechanism of HA production by RPE in HaCaT keratinocytes. As seen in Figure 3A,B, RPE enhanced HA production with no evidence of cytotoxicity. HAS2 expression was dose-dependently increased with RPE (0–80 μg/mL) (Figure 3C). Previous reports indicate that the activation of MAP2K-MAPK signaling could regulate HAS2 expression.[11,25] Similarly, our data shows that RPE substantially increased the phosphorylation of ERK, JNK and p38 (Figure 3D). Likewise, the levels of p-MEK1/2, p-MKK4,

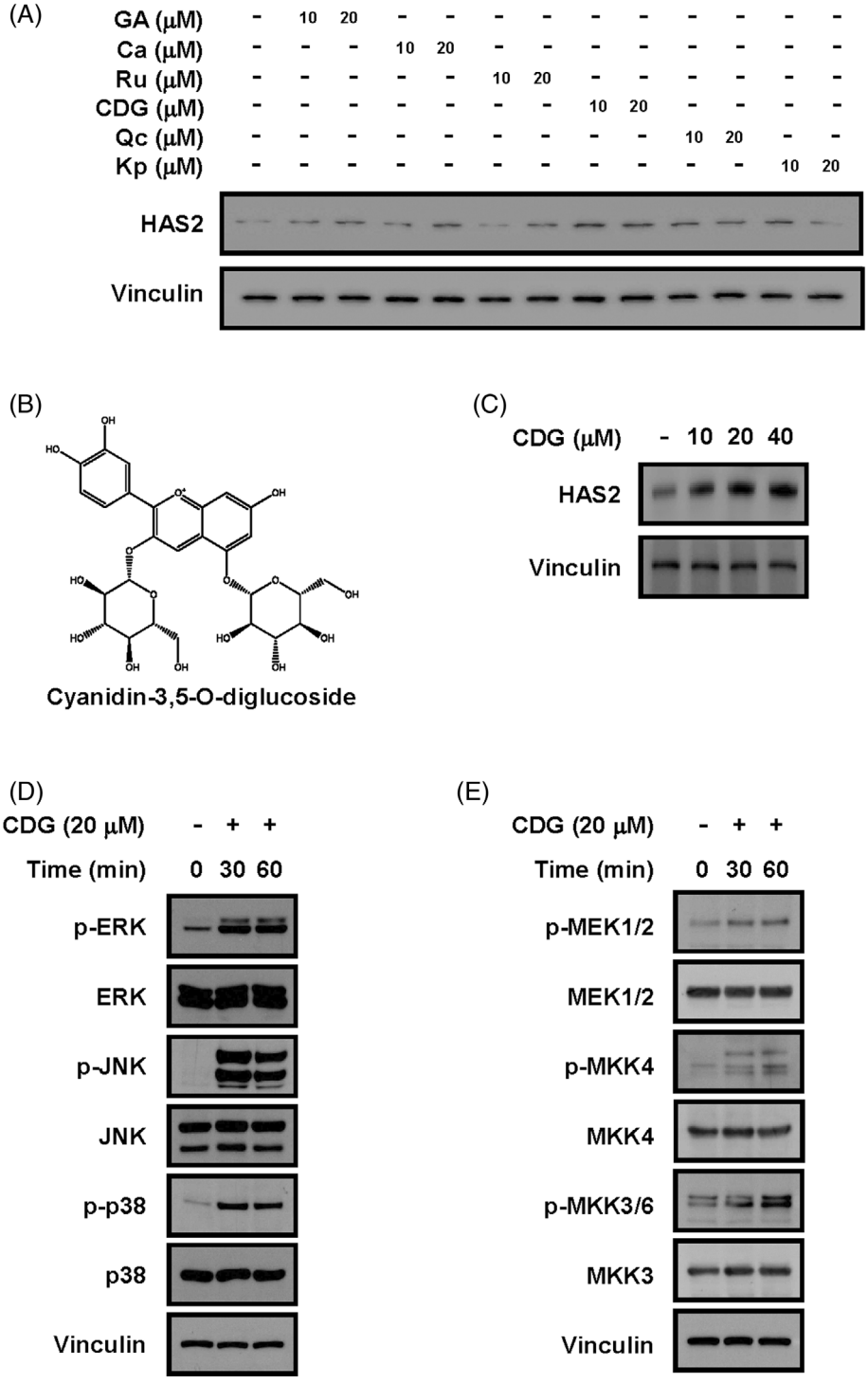

FIGURE 5 Effects of cyanidin-3,5-*O*-diglucoside on HAS2 and MAP2K-MAPK signaling pathways. (A) Effects of different compounds in RPE on HAS2 protein expression in HaCaT cells. Cells were treated with the designated compounds for 3 h. HAS2 and vinculin expression levels in cell lysates were determined by Western blot. (B) Molecular structure of CDG. (C) Effects of CDG on HAS2 protein expression. (D) Effects of CDG on MAPK signaling in HaCaT cells. Protein expression levels of phosphorylated and total ERK, JNK, and p38. (E) Effects of CDG on MAP2K signaling in HaCaT cells. Protein expression levels of phosphorylated and total MAPKs, as determined by Western blot. Vinculin was used as a loading control. CDG, cyanidin-3,5-O-diglucoside; HAS, hyaluronic acid synthase; MAPKs, mitogen-activated protein kinase; RPE, rose petal extract

and p-MKK3/6 were upregulated by 40 and 80 μg/ml RPE (Figure 3E).

3.4 | Analysis of *Rosa Gallica* extract

To identify the active compound associated with the skin hydration effects of RPE, we conducted UPLC coupled with a PDA. A total of six peaks excluding the solvent peak were identified (Table 2). The main components of RPE were gallic acid, catechin (detected at 254 nm), rutin, quercetin, kaempferol (detected at 360 nm), and cyanidin-3,5-*O*-diglucoside (detected at 520 nm).

3.5 | CDG increases HAS2 and activates MAP2K-MAPK signaling pathways

We evaluated the effects of the six compounds identified in RPE on HAS2 expression in HaCaT keratinocytes. In Figure 5A, the HAS2 level was the highest in the CDG-treated cells among all six compounds tested. We, therefore, assumed that CDG (Figure 5B) could be the primary bioactive compound in RPE responsible for eliciting the skin hydration effects. In addition, HAS2 expression was dose-dependently increased by CDG as shown in Figure 5C. Furthermore, CDG (20 μM) activated the MAPK2-MAPK signaling pathway in HaCaT keratinocytes (Figure 5D,E).

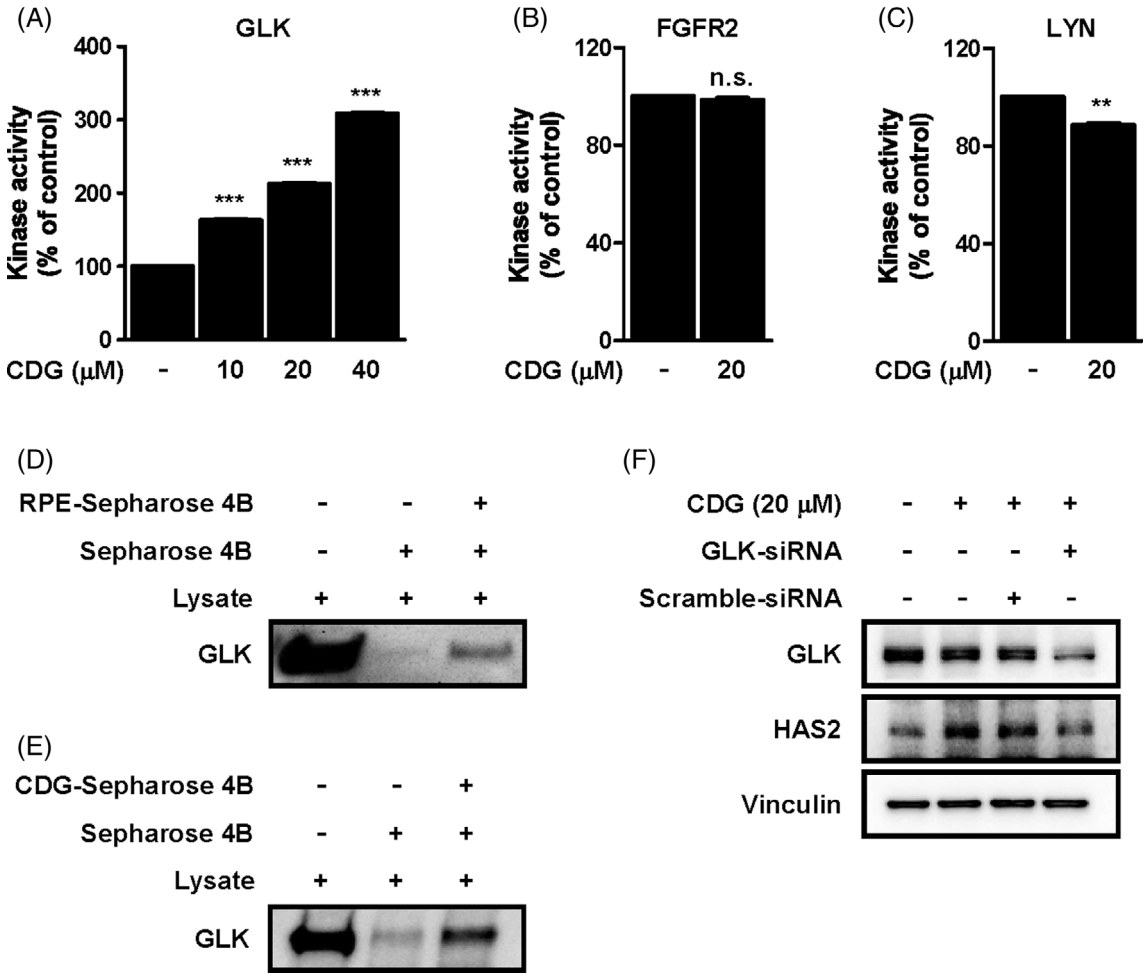

FIGURE 6 Effects of CDG on GLK kinase activity. (A) CDG increases GLK kinase activity. Data shown as mean ± S.D. (B and C) CDG does not inhibit other kinases (FGFR2, LYN) [negative control]. Data shown as mean ± S.D. Kinase activity was assessed by ELISA using cell lysate supernatant. Kinase activity was measured as described in Section 2. (D and E) RPE and CDG binds to GLK in vitro, as determined by pull-down assay. The binding site was detected with immunoblotting. (F) Transfecting GLK with siRNA resulted in a significant knock down of GLK protein expression and attenuated HAS2 expression. ** significant difference of $p < 0.01$ (and ***$p < 0.001$) relative to control. CDG, cyanidin-3,5-O-diglucoside; ELISA, enzyme-linked immunosorbent assay; GLK, germinal-center kinase-like kinase; HAS, hyaluronic acid synthase; MAPKs, mitogen-activated protein kinase; RPE, rose petal extract, siRNA, small interfering RNA

3.6 | CDG upregulates GLK kinase activity

As GLK has been reported to activate MAP2K-MAPK signaling,[13] we sought to investigate a possible link between GLK kinase activity and increased HAS2 production by CDG. GLK kinase activity was measured after treating the cells with CDG, and it was found that the kinase activity was significantly increased (Figure 6A). On the other hand, CDG did not influence FGFR2 and LYN kinase activities, suggesting specificity of CDG against GLK (Figure 6B,C). Moreover, the direct binding of RPE and CDG to GLK protein was observed based on pull-down assays from cell lysates (Figure 6D,E). In addition, silencing of GLK blocked CDG-mediated upregulation of HAS2 levels (Figure 6F), further confirming that GLK is a target protein of CDG.

3.7 | Computational analysis of CDG—GLK interaction

For structural insights into how CDG activates GLK, we investigated the structure of GLK with docking of CDG onto GLK. Most kinases modulate their activity via phosphorylation of their own activation loops, which changes the conformation of the loop and increases enzymatic activity.[26] However, GLK forms a dimer and swaps the activation loop, while phosphorylation increases enzymatic activity (Figure 7A,C).[12] We hypothesized that phosphorylation of the activation loop changes its conformation and dissociates the dimer; in this model, CDG hinders dimer formation, prevents auto-inhibition, and increases the enzymatic activity of GLK (Figure 7B). We further evaluated the possibility of CDG binding on the dimerization interface by docking CDG with GLK. The docking

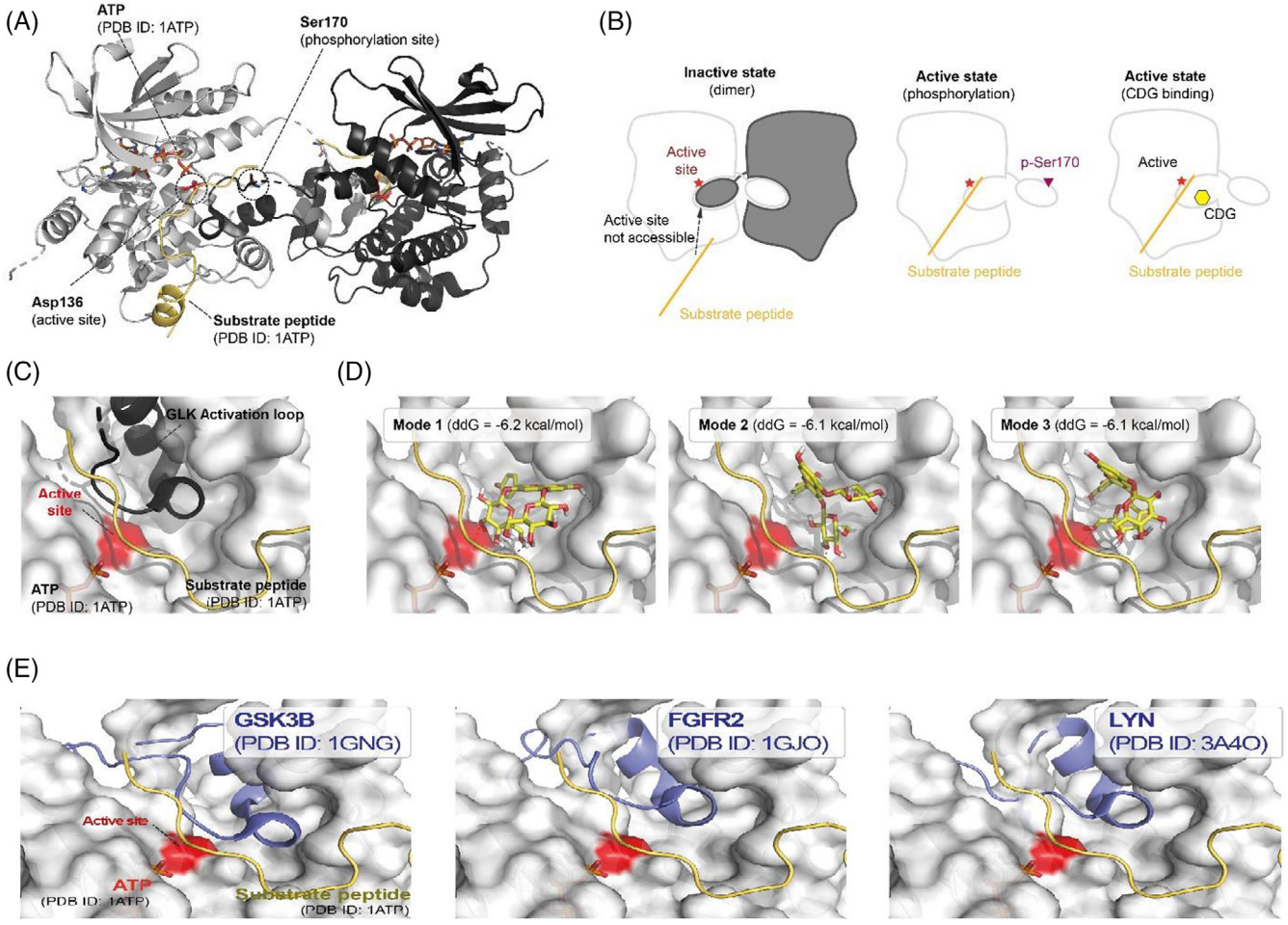

FIGURE 7 Structure of GLK and CDG interaction model. (A) The structures of the crystalline GLK and location of the putative substrate peptide. (B) Schematic model of GLK active, inactive, and CDG-binding forms. (C) Locations of GLK activation loop and putative substrate peptide. (D) Top three highest scoring docking conformations. (E) Location of the activation loop in other kinases. CDG, cyanidin-3,5-O-diglucoside; GLK, germinal-center kinase-like kinase; MAPK, mitogen-activated protein kinase

conformation of CDG demonstrated that its benzopyran moiety can interact with the hydrophobic amino acids of GLK, suggesting that CDG can bind on the GLK dimerization interface (Figure 7D). In contrast, the activation loops of other kinases (GFGR2 and LYN) would not permit CDG binding and therefore CDG would be unlikely to directly interfere with their activities (Figure 7E).

4 | DISCUSSION

Three different isoforms of HAS (HAS1, HAS2, and HAS3) together contribute to synthesis of HA within cells.[28] Although all three HAS isoforms can synthesize high-molecular mass HA, only HAS2 can produce HA at molecular sizes of up to 6000 kDa, the reported average size of most available HA in healthy tissue.[10,29]

Our findings show that RPE markedly increases HAS2 expression in a 3D human skin equivalent model (Figure 2). We used RPE as a moisturizing agent for human skin and evaluated its effects on hydration in a clinical trial and in vitro models. Based on the clinical observations, individuals treated with RPE cream exhibited elevated hydration in the skin when compared to the placebo cream by the end of the trial. A similar study found that a herbal extract cream increased skin hydration in human subjects.[27] The increases in skin hydration in the participants of the present study could be attributable to the elevation of HA levels elicited by RPE in the skin.

The involvement of signaling pathways, including MAPK and MAP2K pathways in HAS production has been reported in previous studies.[7,30] According to Jeon et al., MAPK-specific inhibitors suppressed HAS2 and HAS3 expression leading to a decrease in HA production.[7] Our findings demonstrate that RPE strongly

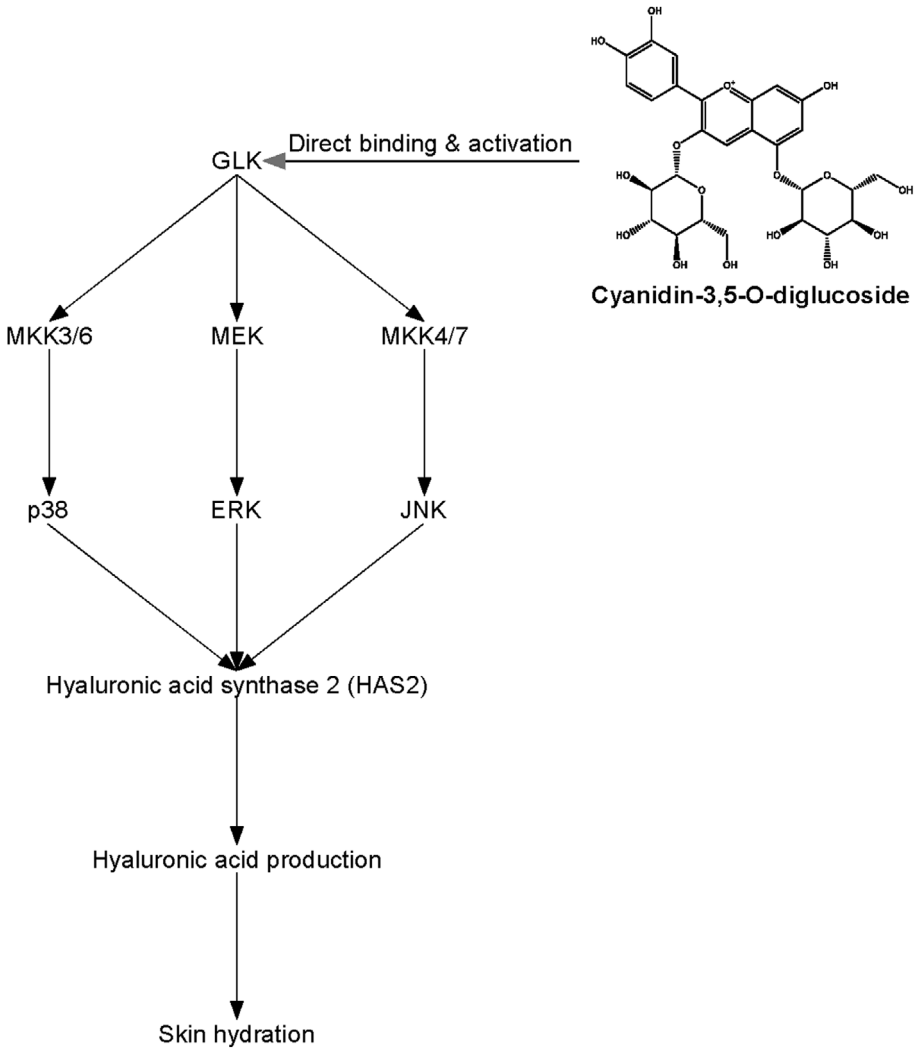

FIGURE 8 Schematic diagram summarizing the GLK-MAP2K-MAPK signaling pathway and its mechanism. GLK, germinal-center kinase-like kinase; MAPK, mitogen-activated protein kinase

phosphorylates intermediaries in the MAP2K/MAPK pathways (Figure 3D,E). We identified CDG as the most active compound that could be responsible for RPE's skin hydration effects based on its efficacy in upregulating HAS2 expression (Figure 4). CDG also substantially increased HAS2 expression and phosphorylated MAP2K/MAPK signaling in human keratinocytes (Figure 5C–E). Furthermore, GLK kinase activity was significantly increased following CDG application (Figure 6), indicating that the HAS2 production could be linked to GLK kinase activity. We found direct binding of CDG with GLK kinase (Figure 6E), suggesting that CDG activates GLK kinase via a direct interaction. Moreover, transfection of siRNA-GLK neutralized the effect of CDG on HAS2 expression (Figure 6F). Taken together, these observations suggest that RPE elicits strong skin hydration effects by increasing the production of HAS2 by activating GLK and phosphorylating MAP2K/MAPK signaling pathways. GLK forms an activation loop-swapping dimer, with the CDG docking model suggesting that CDG may hinder dimer formation and allow the substrate peptide to access the active site (Figure 7). The precise molecular mechanisms involved in CDG-induced activation will be examined in further studies.

5 | CONCLUSION

In conclusion, RPE demonstrated remarkable skin moisturizing activities by stimulating HA synthesis. The improvement of skin hydration in the human subjects with RPE treatment was noteworthy. This study has highlighted that the enhancement of HA synthesis was linked with GLK kinase activity and the phosphorylation of MAP2K/MAPK signaling pathways (Figure 8). Therefore, GLK could be a potential target to increase HA production in the skin. Based on our findings, we suggest that the skin hydration effects of RPE are attributable to CDG. Further investigation of its potential application as a skin moisturizing agent are recommended.

AUTHOR CONTRIBUTIONS

Ji-Won Seo: Investigation, Writing—original draft, Formal analysis. **Seongin Jo**: Investigation, Methodology, Formal analysis. **Young Sung Jung**: Investigation, Formal analysis. **Mohammad-Al Mijan**: Investigation. **Joy Cha**: Investigation. Seungpyo Hong: Software, Formal analysis. **Sanguine Byun**: Validation, Writing—review & editing, Supervision, Funding acquisition. **Tae-Gyu Lim**: Validation, Writing—review & editing, Supervision, Funding acquisition. The final manuscript has been read and approved by all the authors.

ACKNOWLEDGMENTS

This work was supported by the National Research Foundation of Korea (NRF) grant funded by the Korean Government (Ministry of Science, ICT and Future Planning) [2020R1A2C1010703], Korea Institute of Planning and Evaluation for Technology in Food, Agriculture and Forestry (IPET) through Technology Commercialization Support Program, funded by Ministry of Agriculture, Food and Rural Affairs (MAFRA) (821018f3), and the Ministry of Small and Medium-sized Enterprises (SMEs) and Startups (MSS), Korea, under the "Regional Specialized Industry Development Plus Program (R&D, S3094265)" supervised by the Korea Institute for Advancement of Technology (KIAT).

CONFLICT OF INTEREST

The authors declare no conflict of interests.

DATA AVAILABILITY STATEMENT

Data sharing not applicable—no new data generated, or the article describes entirely theoretical research Data sharing not applicable to this article as no datasets were generated or analysed during the current study

ETHICS STATEMENT

All procedures performed in studies involving human participants were in accordance with the ethical standards of the institutional and/or national research committee and with the 1964 Helsinki declaration and its later amendments or comparable ethical standards. Approved by the local medical ethics committee (permit number KIDS-BTE003-SJU) and conducted following the principles of the Declaration of Helsinki.

ORCID

Tae-Gyu Lim https://orcid.org/0000-0001-6930-9565

ORCID

Tae-Gyu Lim https://orcid.org/0000-0001-6930-9565

REFERENCES

1. Mojumdar EH, Pham QD, Topgaard D, Sparr E. Skin hydration: interplay between molecular dynamics, structure and water uptake in the stratum corneum. Sci Rep. 2017;7:15712. https://doi.org/10.1038/s41598-017-15921-5
2. Dmitrieva NI, Burg MB. Increased insensible water loss contributes to aging related dehydration. PLoS One. 2011;6:e20691. https://doi.org/10.1371/journal.pone.0020691
3. Purnamawati S, Indrastuti N, Danarti R, Saefudin T. The role of moisturizers in addressing various kinds of dermatitis: a review. Clin Med Res. 2017;15:75–87. https://doi.org/10.3121/cmr.2017.1363
4. Campiche R, Jackson E, Laurent G, Roche M, Gougeon S, Séroul P, et al. Skin filling and firming activity of a hyaluronic

acid inducing synthetic tripeptide. Int J Pept Res Ther. 2020;26:181–9. https://doi.org/10.1007/s10989-019-09827-1

5. Dong Q, Guo X, Li L, Yu C, Nie L, Tian W, et al. Understanding hyaluronic acid induced variation of water structure by near-infrared spectroscopy. Sci Rep. 2020;10:1387. https://doi.org/10.1038/s41598-020-58417-5
6. Stern R. In: Farage MA, Miller KW, Maibach HI, editors. Textbook of aging skin. Berlin, Heidelberg: Springer; 2010. p. 225–38. https://doi.org/10.3892/ijmm.2015.2121
7. Lim TG, Jeon AJ, Yoon JH, Song D, Kim JE, Kwon JY, et al. 20-O-β-D-glucopyranosyl-20(S)-protopanaxadiol, a metabolite of ginsenoside Rb1, enhances the production of hyaluronic acid through the activation of ERK and Akt mediated by Src tyrosin kinase in human keratinocytes. Int J Mol Med. 2015;35:1388–94. https://doi.org/10.3892/ijmm.2015.2121
8. Yao Q, Jia T, Qiao W, Gu H, Kaku K. Unsaturated fatty acid-enriched extract from Hippophae rhamnoides seed reduces skin dryness through up-regulating aquaporins 3 and hyaluronan synthetases 2 expressions. J Cosmet Dermatol. 2021;20:321–9. https://doi.org/10.1111/jocd.13482
9. Siiskonen H, Oikari S, Pasonen-Seppänen S, Rilla K. Hyaluronan synthase 1: a mysterious enzyme with unexpected functions. Front Immunol. 2015;6:43. https://doi.org/10.3389/fimmu.2015.00043
10. Wang Y, Lauer ME, Anand S, Mack JA, Maytin EV. Hyaluronan synthase 2 protects skin fibroblasts against apoptosis induced by environmental stress. J Biol Chem. 2014;289:32253–65. https://doi.org/10.1074/jbc.M114.578377
11. Rauhala L, Jokela T, Kärnä R, Bart G, Takabe P, Oikari S, et al. Extracellular ATP activates hyaluronan synthase 2 (HAS2) in epidermal keratinocytes via P2Y2, Ca2+ signaling, and MAPK pathways. Biochem J. 2018;475:1755–72. https://doi.org/10.1042/bcj20180054
12. Marcotte D, Rushe M, Lukacs MARC, Atkins K, Sun X, Little K, et al. Germinal-center kinase-like kinase co-crystal structure reveals a swapped activation loop and C-terminal extension. Protein Sci. 2017;26:152–62. https://doi.org/10.1002/pro.3062
13. Chuang H-C, Tan T-H. MAP4K3/GLK in autoimmune disease, cancer and aging. J Biomed Sci. 2019;26:82. https://doi.org/10.1186/s12929-019-0570-5
14. Fukada M, Kano E, Miyoshi M, Komaki R, Watanabe T. Effect of "Rose Essential Oil" inhalation on stress-induced skin-barrier disruption in rats and humans. Chem Senses. 2011;37:347–56. https://doi.org/10.1093/chemse/bjr108
15. Lee M-H, Nam TG, Lee I, Shin EJ, Han A-R, Lee P, et al. Skin anti-inflammatory activity of rose petal extract (*Rosa gallica*) through reduction of MAPK signaling pathway. Food Sci Nutr. 2018;6:2560–7. https://doi.org/10.1002/fsn3.870
16. Song YR, Lim WC, Han A, Lee MH, Shin EJ, Lee KM, et al. Rose petal extract (*Rosa gallica*) exerts skin whitening and anti-skin wrinkle effects. J Med Food. 2020;23:870–8. https://doi.org/10.1089/jmf.2020.4705
17. Jo S, Jung YS, Cho YR, Seo JW, Lim WC, Nam TG, et al. Oral administration of *Rosa gallica* prevents UVB-induced skin aging through targeting the c-Raf signaling axis. Antioxidants (Basel). 2021;10:1663. https://doi.org/10.3390/antiox10111663
18. Park G, Baek S, Kim JE, Lim TG, Lee CC, Yang H, et al. Flt3 is a target of coumestrol in protecting against UVB-induced skin photoaging. Biochem Pharmacol. 2015;98:473–83. https://doi.org/10.1016/j.bcp.2015.08.104
19. Jo S, Samarpita S, Lee JS, Lee YJ, Son JE, Jeong M, et al. 8-Shogaol inhibits rheumatoid arthritis through targeting TAK1. Pharmacol Res. 2022;178:106176. https://doi.org/10.1016/j.phrs.2022.106176
20. Kim JH, Lee JE, Kim T, Yeom MH, Park JS, di Luccio E, et al. 7,3′,4′-Trihydroxyisoflavone, a metabolite of the soy isoflavone daidzein, suppresses α-melanocyte-stimulating hormone-induced melanogenesis by targeting melanocortin 1 receptor. Front Mol Biosci. 2020;7:577284. https://doi.org/10.3389/fmolb.2020.577284
21. Berman HM, Westbrook J, Feng Z, Gilliland G, Bhat TN, Weissig H, et al. The Protein Data Bank. Nucleic Acids Res. 2000;28:235–42. https://doi.org/10.1093/nar/28.1.235
22. Kim S, Chen J, Cheng T, Gindulyte A, He J, He S, et al. PubChem in 2021: new data content and improved web interfaces. Nucleic Acids Res. 2021;49:D1388–95. https://doi.org/10.1093/nar/gkaa971
23. Morris GM, Huey R, Lindstrom W, Sanner MF, Belew RK, Goodsell DS, et al. AutoDock4 and AutoDockTools4: automated docking with selective receptor flexibility. J Comput Chem. 2009;30:2785–91. https://doi.org/10.1002/jcc.21256
24. Trott O, Olson AJ. AutoDock Vina: improving the speed and accuracy of docking with a new scoring function, efficient optimization, and multithreading. J Comput Chem. 2010;31:455–61. https://doi.org/10.1002/jcc.21334
25. Ducale AE, Ward SI, Dechert T, Yager DR. Regulation of hyaluronan synthase-2 expression in human intestinal mesenchymal cells: mechanisms of interleukin-1β-mediated induction. Am J Physiol Gastrointest Liver Physiol. 2005;289:G462–70. https://doi.org/10.1152/ajpgi.00494.2004
26. Adams JA. Activation loop phosphorylation and catalysis in protein kinases: is there functional evidence for the autoinhibitor model? Biochemistry. 2003;42:601–7. https://doi.org/10.1021/bi020617o
27. Roh SS, Choi I, Kim HM, Lee MS, Jin MH, Kim BH, et al. Clinical efficacy of herbal extract cream on the skin hydration, elasticity, thickness, and dermis density for aged skin: a randomized controlled double-blind study. J Cosmet Dermatol. 2019;18:1389–94. https://doi.org/10.1111/jocd.12846
28. Stern R, Maibach HI. Hyaluronan in skin: aspects of aging and its pharmacologic modulation. Clin Dermatol. 2008;26:106–22. https://doi.org/10.1016/j.clindermatol.2007.09.013
29. Cowman MK. In: Baker DC, editor. Advances in carbohydrate chemistry and biochemistry. CA, USA: Academic Press Inc Elsevier Science; 2017. p. 1–59. https://doi.org/10.1016/bs.accb.2017.10.001
30. Choi E, Kang YG, Hwang SH, Kim JK, Hong YD, Park WS, et al. In vitro effects of dehydrotrametenolic acid on skin barrier function. Molecules. 2019;24:4583. https://doi.org/10.3390/molecules24244583

How to cite this article: Seo J-W, Jo S, Jung YS, Mijan M-A, Cha J, Hong S, et al. *Rosa gallica* and its active compound, cyanidin-3,5-*O*-diglucoside, improve skin hydration via the GLK signaling pathway. BioFactors. 2022. https://doi.org/10.1002/biof.1922